

Demystifying generalized parton distributions

A. Freund

Institut für Theoretische Physik, Universität Regensburg, 93040 Regensburg, Germany

Received: 2 December 2002 / Revised version: 20 August 2003 /
Published online: 2 October 2003 – © Springer-Verlag / Società Italiana di Fisica 2003

Abstract. In this paper, I will explain in as simple and intuitive physical terms as possible what generalized parton distributions are, what new information about the structure of hadrons they convey and therefore what picture of the hadron will emerge. To develop this picture, I will use the example of deeply virtual Compton scattering (DVCS) and exclusive meson electroproduction processes. Based on this picture, I will then make some general predictions for these processes.

1 Introduction

Scientists have striven for centuries to unravel the dynamics and the structures involved in the physical systems they have been investigating, from large scale structures in our universe over biological systems down to the smallest scales achievable in today's high energy experiments. At these smallest scales the questions one is trying to answer are "What are the substructures of hadrons, what are the dynamics of these substructures and what three dimensional picture of hadrons is emerging?"

In the theory of strong or color interactions (QCD) parton distribution functions (PDFs) encode the long distance or bound state i.e. non-perturbative information about hadrons. These PDFs are precisely what we need in order to construct a dynamical as well as geometrical picture of these objects. Unfortunately, most high energy experiments analyzing hadronic substructure study inclusive reactions such as deep inelastic scattering (DIS) $e + p \rightarrow e + X$; in other words the object they would like to study is destroyed in the reaction. Although PDFs can be extracted from inclusive data, these functions are only single particle distributions precisely because the target is destroyed and, hence, they depend only on a longitudinal momentum fraction, x_{Bj} , and a transverse resolution scale, μ^2 . Since inclusive PDFs do not contain information on the impact parameter of the probe, vital information about the three dimensional distribution of substructure is lost and, therefore, these PDFs can only give a one dimensional picture of a hadron. It could be argued that so-called unintegrated PDFs (see for example [1]) contain more information on hadrons, since the additional transverse scale can be interpreted as a relative transverse position. However, this scale is integrated over in physical observables and thus no direct information can be deduced from it. In order to gain insight into a hadron's three dimensional structure one has to measure particle correlation functions which encode additional information on how the object as

a whole reacts to an outside probe in terms of physical observables. Correlations in hadrons refer to the dynamical influence during the reaction one or more particles or partons found in a particular state inside the hadron have on one or more other partons found in a different state inside the same hadron. A good example would be the transition of a quark/gluon of a certain momentum into a configuration inside the same hadron with a different momentum or the removal from the hadron i.e. transition into vacuum, of a $q\bar{q}$ /gluon pair with a certain momentum configuration. Because of the closeness in meaning between parton correlation and parton configuration, I will use the two phrases interchangeably from now on. Note that particle correlation functions can only be measured if the hadron stays intact during and after the reaction since the dynamical relationship between the different partons would otherwise be destroyed. This can only be achieved if no large color forces, responsible for a break-up, occur during the reaction. This requirement forces such a reaction to be mediated by color neutral objects such as color singlets or, at the very least, requires that color is locally saturated. The experimental signature of such a process can be either a so-called rapidity gap meaning that the produced particles which are well localized in the detector, are clearly separated from the intact final state hadron with no detector activity in between the two, or a small so-called missing mass, which characterizes the difference between the initial energy and the sum of the energies of all the reconstructed particles in the detector. There are many reactions of this kind, such as hard diffraction $e + p \rightarrow e + p + X$ or, in particular, deeply virtual Compton scattering (DVCS) $e + p \rightarrow e + p + \gamma$ [2–7] which is the most exclusive example of hard diffraction. Hard is meant here in the sense of the presence of a large scale in the reaction such as a large momentum transfer from probe to target. In the perturbative QCD description of fully exclusive hard reactions such as DVCS, we finally encounter the objects we have been looking for: particle

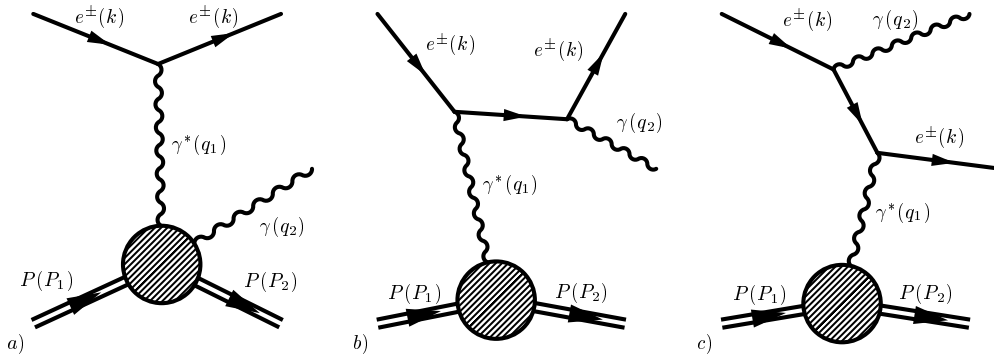


Fig. 1. **a** DVCS graph, **b** Bethe–Heitler process with photon from final state lepton and **c** with photon from initial state lepton

correlation functions. They appear in the collinear factorization theorems of these reactions [6, 8] where “collinear” refers to the physics being dominated by what is happening on the light cone neglecting internal transverse momenta. Factorization theorems state that, within QCD, one can factorize the leading term in the cross section or scattering amplitude of a particular hard reaction to all orders in perturbation theory into a convolution of a finite or infra-red safe, hard scattering function and an infrared sensitive, non-perturbative function, a PDF. The remaining terms in the cross section or amplitude are suppressed in the large scale of the reaction and can be disregarded, at least in the limit of very large scales. The hard scattering function is particular to each reaction but computable to all orders in perturbation theory. The PDFs which are universal objects and can be used in other hard, exclusive reactions, cannot be computed within perturbative QCD save for their momentum scale dependence induced by the renormalization of the theory. They are given, in a quantum field theoretic language, as a Fourier transformation of a matrix element of non-local, renormalized, operators. The key thing, in this context, are the in and out states of these matrix elements. In inclusive reactions such as DIS, the in and out states are the same, since the scattering amplitude can be directly related through the optical theorem to a reaction which has the same in and out state. In hard, exclusive reactions the in and out state differ, at least, in their momenta. This is due to a finite momentum transfer in the t -channel of the reaction onto the outgoing hadron, most commonly a nucleon. These PDFs depend on more variables, namely those characterizing the momentum difference of the in and out state, than the PDFs in inclusive reactions which only depend on one momentum variable, apart from the momentum scale dependence and therefore carry only one dimensional information on the hadron. The behavior of these PDFs, called generalized parton distributions (GPDs) [2–5, 9, 10], under a change of their variables encodes the response of the entire hadron, i.e. its substructure, to the outside probe. Therefore, these GPDs are particle correlation functions, more precisely light cone particle correlation functions, and a complete mapping in all their variables through experiments would give us for the first time a full three dimensional picture of hadrons. Please note here that GPDs are by no means the only particle correlation functions encountered in high en-

ergy reactions. For example, so called, higher twist matrix elements in DIS, which contain more than just two elementary operators, are correlation functions since the momenta of the third, fourth etc. operator in the matrix element depend on the momenta of the other operators involved. Furthermore, generalized distribution amplitudes [11–13] encountered in exclusive $\gamma\gamma^*$ reactions or transition GPDs in, for example, $e + p \rightarrow e + n + \pi^+$ are also correlation functions (for a review see [12] and references therein). Since the aim of this paper is not completeness but rather an intuitive understanding of at least some of the physics involved, we will only discuss the afore-mentioned GPDs and their physical implications.

In order to directly extract GPDs from experiment one has to access scattering amplitudes. Unfortunately, the cross section for exclusive processes is the amplitude times its complex conjugate, $|A|^2$, compared to inclusive processes where the cross section is just given by the imaginary part of the amplitude. Though we are accessing both the real and the imaginary part of the amplitude in exclusive processes, their phase structure i.e. each part individually, cannot be cleanly separated unless there is a “phase filter”. A “phase filter” would be a well understood process with which the exclusive reaction interferes. Fortunately, there is such a process in the case of DVCS, the QED Compton or Bethe–Heitler (BH) process (see Fig. 1), first discussed in [14]. The interference term between the two processes allows one to directly access both the imaginary and the real part of the DVCS scattering amplitude which contain, *simultaneously*, four distinct structures, namely \mathcal{H} , an unpolarized amplitude with no hadron spin-flip, \mathcal{E} , a polarized amplitude with no hadron spin-flip, \mathcal{H}' , an unpolarized amplitude with hadron spin-flip and \mathcal{E}' , a polarized amplitude with hadron spin-flip. The imaginary part is accessible through the measurement of the beam spin asymmetry (longitudinal polarization in and opposite to the beam direction) also called single spin asymmetry (SSA) and the real part through the beam charge asymmetry (reversal of the lepton charge) or simply called charge asymmetry (CA) [7, 15, 16]. This “filtering” has been aptly named “nucleon holography” by the authors of [17], since it employs the same principle of interference as regular holography. Note that the nucleon spin-flip is only made possible because of a finite momentum transfer t onto the final state nucleon as compared to DIS where $t = 0$ and

thus there is no spin-flip. This last statement means that \mathcal{E} and $\tilde{\mathcal{E}}$ have no inclusive analog and hence contain unique information on the nucleon only accessible in exclusive reactions.

Note, furthermore, that whereas on the amplitude level we have “nucleon holography”, on the deep structure level of the GPDs we will, as I will explain in a later section, have “nucleon tomography” [18] (see also [19]), since for each value of x_{Bj} and each value of t we are studying the dynamics of a slice of a nucleon and so, when we put all of the slices together we obtain a three dimensional image of a nucleon, as one obtains a three dimensional image of a person when putting enough MRI pictures together.

In Sect. 2, I will define GPDs and then develop a picture of what they mean in an intuitive way based on the example of DVCS and exclusive meson production. In Sec. 3, I will make general predictions about DVCS in particular and hard exclusive reactions in general at facilities such as the planned EIC at BNL, the proposed HERA III or a dedicated fixed target experiment. I will then conclude in Sec. 4.

2 What is the physical picture GPDs convey?

2.1 GPD definition

Whenever I will talk about GPDs in the following, I will refer to GPDs in a nucleon, since I will mainly concern myself with hard electroproduction reactions involving protons. However, the statements below are much more general in nature and apply to any hadron target. For brevity and ease of presentation, I will restrict myself to nucleons.

GPDs, first implicitly introduced in [2] and later rediscovered in [3, 5], are generally defined through the Fourier transform of matrix elements of renormalized, non-local twist-two operators. Twist-two operators are composite operators containing only two elementary fields of the theory. These are situated at different positions on a light ray making them non-local and are sandwiched between *unequal* momentum nucleon states. The essential feature of such light cone parton correlation functions, where the difference in the in and out state is responsible for the correlations, is the presence of a finite momentum transfer, $\Delta = p - p'$, in the t -channel (p, p' are the initial and final state nucleon momenta). Hence, the partonic structure of the nucleon is tested at *distinct* momentum fractions.

There are many representations of GPDs [2, 3, 5, 20, 21]. In this paper I will use the off-diagonal PDFs, $\mathcal{F}^i(X, \zeta)$, defined by Golec-Biernat and Martin [20] and used in the numerical solution of the renormalization group or evolution equations in [22] (for other treatments see [20, 21, 23, 24]). This representation will allow us a very intuitive insight into GPDs as I will explain now.

The GPDs in this representation depend on the momentum fraction $X \in [0, 1]$ of the *incoming* proton’s momentum, p , and the skewedness variable $\zeta = \Delta^+ / p^+$ (so that $\zeta = x_{Bj}$ for DVCS and meson production). This is analogous to the case of forward PDFs where x_{Bj} is also defined with respect to the incoming proton’s momentum.

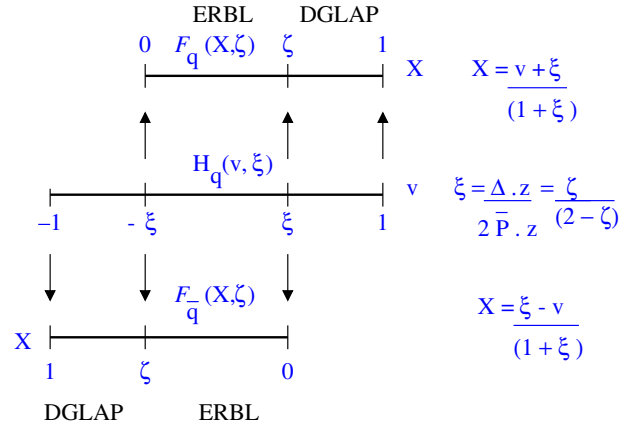


Fig. 2. The relationship between $\mathcal{F}^q(X, \zeta)$, $\mathcal{F}^{\bar{q}}(X, \zeta)$ and $H^q(x, \xi)$ with $x \in [-1, 1]$ and $X \in [0, 1]$

For the quark case, the relationship of the quark and anti-quark distributions, $\mathcal{F}^q(X, \zeta)$, $\mathcal{F}^{\bar{q}}(X, \zeta)$, to the more widely used $H^q(x, \xi)$ [3] where the GPDs are defined with respect to the average of p and p' ($x \in [-1, 1]$ and $\xi = \zeta / (2 - \zeta) \in [0, 1]$) is shown in Fig. 2. More explicitly, for $x \in [-\xi, 1]$:

$$\mathcal{F}^{q,a} \left(X = \frac{x + \xi}{1 + \xi}, \zeta \right) = \frac{H^{q,a}(x, \xi)}{1 - \zeta/2}, \quad (1)$$

and for $x \in [-1, \xi]$

$$\mathcal{F}^{\bar{q},a} \left(X = \frac{\xi - x}{1 + \xi}, \zeta \right) = -\frac{H^{q,a}(x, \xi)}{1 - \zeta/2}. \quad (2)$$

The two distinct transformations between x and X for the quark and anti-quark cases are shown explicitly on the left hand side of (1) and (2). There are two distinct regions: the DGLAP region, $X > \zeta$ ($|x| > \xi$), in which the GPDs behave like regular parton distributions and obey a generalized form of the so-called DGLAP equations for PDFs, and the so-called ERBL region, $X < \zeta$ ($|x| < \xi$), where the GPDs behave like distributional amplitudes/meson wavefunctions and obey a generalized form of the ERBL equations for distributional amplitudes [20–24]. In the ERBL region, due to the fermion symmetry, \mathcal{F}^q and $\mathcal{F}^{\bar{q}}$ are not independent anymore. In fact $\mathcal{F}^q(X, \zeta) = -\mathcal{F}^{\bar{q}}(\zeta - X, \zeta)$, which leads to an anti-symmetry of the unpolarized quark singlet distributions (summed over flavor a), $\mathcal{F}^S = \sum_a \mathcal{F}^{q,a} + \mathcal{F}^{\bar{q},a}$, which is C -even, about the point $\zeta/2$ (the \bar{C} -odd non-singlet and the C -even gluon, \mathcal{F}^g , which is built from $xH^g(x, \xi)$, are symmetric about this point). For a detailed review of the mathematical properties see, for example, [4].

The operator definition of the \mathcal{F} ’s is analogous to the one for the H ’s:

$$\begin{aligned} & \mathcal{F}^q(X, \zeta) \\ &= \int \frac{dz^-}{4\pi} e^{-i(X-\zeta)p^+z^-} \langle p | \bar{\psi}(z^-) \mathcal{P} \gamma^+ \psi(0) | p' \rangle, \\ & \mathcal{F}^g(X, \zeta) \end{aligned} \quad (3)$$

$$= \int \frac{dz^-}{2\pi X p^+} e^{-i(X-\zeta)p^+ z^-} \langle p | G_{+\nu}(z^-) \mathcal{P} G_{+}^\nu(0) | p' \rangle,$$

except that the Fourier conjugate momentum fraction, the light cone positions and the momenta of the in and out states are different compared to the symmetric approach. Note that one could have, more conventionally, chosen X to be the Fourier conjugate momentum to z^- . Since the crucial points $X = 0$ and $X = \zeta$ are related via the above symmetry arguments, it does not matter whether one chooses one or the other. Nonetheless, the variable $X - \zeta$ will prove convenient later on since it will be zero for $X = \zeta$ which is a special point and signals that large, strictly speaking infinite, light-like separations of the operators will play a very important role in the GPD. As we will see below, this point in the GPD is of paramount importance in hard exclusive reactions like DVCS and meson production. In the symmetric representation [3], the uniqueness of this point in terms of separation of operators on the light ray is not as obvious and thus I prefer a representation here where the uniqueness of this point is directly apparent. This does not mean that one representation is better than another but rather that sometimes one representation is more convenient to use than another.

Below, I will refer quite often to valence and sea quark distributions. In terms of (3) the valence or C -odd non-singlet quark distribution of a flavor a is defined as

$$\mathcal{F}_{\text{val}}^a = \mathcal{F}^{q,a} - \mathcal{F}^{\bar{q},a} \quad (4)$$

such that the first moment in X , summed over all flavors, yields the number of quarks in the proton, and the definition of singlet quark distribution for a given flavor a , a C -even GPD combination, is

$$\mathcal{F}^{S,a} = \mathcal{F}^{q,a} + \mathcal{F}^{\bar{q},a}, \quad (5)$$

which gives the sea quark distribution of flavor a

$$\mathcal{F}_{\text{sea}}^{q,a} = \frac{1}{2} [\mathcal{F}^{S,a} - \mathcal{F}_{\text{val}}^a] = \mathcal{F}_{\text{sea}}^{\bar{q},a}. \quad (6)$$

Note that in the ERBL region, as pointed out above, the quark and anti-quark distributions are not independent from one another anymore and one can only speak of non-singlet and singlet distributions per flavor a without being able to separate out the sea.

2.2 Why does DVCS help us understand GPDs better?

The first question one has to answer is: Why is it that DVCS (see Fig. 1) is the cleanest process within which to measure GPDs in a nucleon? The reason for this is quite simple. With a real photon, one has an elementary, point-like particle in the final state rather than a bound state like a meson or an even more complicated state like several mesons/hadrons or jets adding other unknown, non-perturbative functions. Note that the contribution of the non-point-like part of the real photon wave function which is similar to a meson wavefunction, is power suppressed in

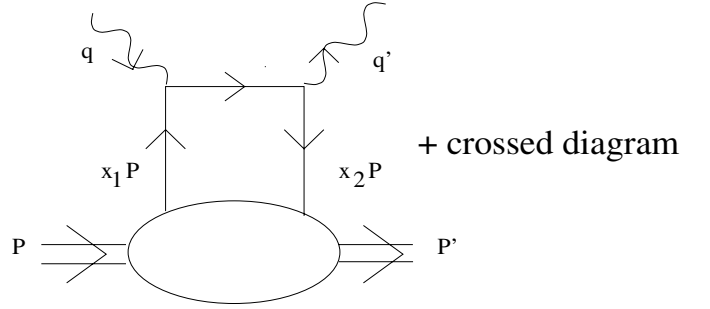


Fig. 3. LO handbag diagram for DVCS. Here $x_1 = X$ and $x_2 = X - \zeta$

DVCS [5,6]. The factorization theorem for the DVCS scattering amplitude [5,6] is merely a simple convolution of a hard scattering function with only *one* GPD rather than with a GPD plus another non-perturbative function as in meson production. To be more precise, DVCS is only sensitive to a charge weighted C -even GPD combination ($\sum_a e_a^2 \mathcal{F}^{S,a} = \sum_a e_a^2 (\mathcal{F}^{q,a} + \mathcal{F}^{\bar{q},a})$) in leading order (LO) of perturbation theory (the gluon GPD enters only in next-to-leading order (NLO)), which is the flavor sum over the singlet quark distribution for a given flavor a . Hence, DVCS does not discriminate between different quark flavors as for example exclusive π^0 production does due to its quark content specific final state.

The DVCS amplitude is $\mathcal{T} \simeq \text{Im} \mathcal{T} \propto \sum_a e_a^2 \mathcal{F}^{S,a}(\zeta, \zeta, Q^2)$ in LO (see for example [2,3,5]). This is true up to $\zeta = x_{Bj} \simeq 0.2-0.3$ even when taking NLO effects into account [15,16,25,26]. Hence, DVCS is dominated, at least in a very broad region of phase space, by the crossover point between the DGLAP and ERBL region. At this particular point in phase space, $X = \zeta$, the parton line carrying momentum fraction x_2 in Fig. 3 is becoming “soft” and all the momentum is carried by the incoming quark with fraction $x_1 = X = \zeta$. Also note that the quark connecting the two photon vertices, which is usually hard i.e. has a large virtuality, is on or almost on mass shell and carries only a large $-$ momentum (see again Fig. 3). Factorization for DVCS still holds in this situation [6], with the hard interaction now being the photon-quark vertex, however, the point $X = \zeta$ in the GPD is indeed rather peculiar. One should recall that the GPD is defined by a Fourier transform of a non-local matrix element on a light ray and that the Fourier conjugate variables are the light-ray separations z^- between operators and a momentum fraction variable. Here this is either X or $X - \zeta$ (see (3)). This means then that for $X - \zeta \rightarrow 0$, $z^- \rightarrow \infty$, and therefore the operators have an infinite separation on the light ray or more physically speaking that there is bad resolution of the probed object in the $-$ direction on the light cone. This situation is analogous to inclusive DIS in the limit of $x_{Bj} \rightarrow 0$. Thus inclusive scattering at small x_{Bj} and DVCS up to a large x_{Bj} in or, at least, near the valence region ($\mathcal{F}_{\text{val}}^a > \mathcal{F}_{\text{sea}}^a$) is dominated by the same type of particle configurations with the only difference being that the configurations in DVCS remain correlated since the proton stays intact! What does the last statement mean from a physical point of view?

2.3 The physical picture of DVCS and its connection to GPDs

The answer to the last question in Sect. 2.2 is simply: The particle configurations/correlations dominating the DVCS cross section are much bigger, in their extension on the light ray, than the probed object itself. Since the produced photon is a point-like object these particle configurations, which one would normally call “end-point” contributions, are not suppressed as in, for example, a meson wave function describing an object of “finite” size¹! This suggests that even in the valence region, one is not probing the actual bound quark structure of both valence and sea but rather QCD vacuum fluctuations as influenced by and interacting with this bound state quark structure. By QCD vacuum fluctuations, I refer to the existence of two separate contributions, a non-perturbative and a perturbative one. The perturbative QCD vacuum fluctuations will be discussed in detail in Sect. 2.4 when I discuss the origin of the dominant parton configurations in DVCS, and the non-perturbative QCD vacuum fluctuations can best be described as the spontaneous fluctuation of color fields into $q\bar{q}$ pairs as well as the formation of topological non-trivial color field structures like instantons [27].

Note a caveat here, though: The operators are not literally separated by an infinite light-like distance, this would only be true in the limit $Q^2 \rightarrow \infty$, but rather by a distance which is inversely proportional to, at most, $X - \zeta = \zeta \frac{\Lambda_{\text{QCD}}^2}{Q^2}$ [28] which acts as a lower bound and is motivated by considering the fact that the intermediate quark in Fig. 3 is not exactly on mass shell. To be definite compare this to DIS at $x_{\text{Bj}} = 0.2$ and an initial, non-perturbative, scale $Q_0^2 = 1 \text{ GeV}^2$. $X - \zeta = X - x_{\text{Bj}}$ would then be bounded by $0.2 \cdot (0.2)^2 / 1 = 0.008$, which is not too small but still 2.5 times smaller, and at $Q^2 = 5 \text{ GeV}^2$, 125 times smaller, than the respective momentum fractions encountered in DIS. The basic claim is: *DVCS probes a larger, light-like distance than DIS for the same x_{Bj} .*

There is a very intuitive picture of why the above interpretation is indeed true and one is not really probing the actual non-perturbative bound state structure of the proton within DVCS but rather the quark and gluon configurations which are not relevant for the bound state. Consider the following situation (Fig. 4) at a low momentum scale Q : In the infinite momentum frame, the proton is moving along the $+$ direction of the light cone i.e. in the positive z or $+z$ direction with each bound state quark carrying on average a momentum fraction, $X \simeq O(0.1) \simeq x_{\text{Bj}}$. If such a quark were to be struck by a virtual photon which has large $+$ ($-x_{\text{Bj}}P_+$) and ($-Q^2/2x_{\text{Bj}}P_+$) components with $P_+ \simeq O(Q)$, it would then only have a large $-$ component but a quasi-zero $+$ component since $X \simeq x_{\text{Bj}}$. This means that the struck quark would have a large momentum in the $-z$ direction, opposite to that of the other

¹ The endpoints, $x = 0$ or $x = 1$, where the asymptotic pion wave function $6x(1-x)$ vanishes, corresponds to an infinite light-like separation of the operators in the associated matrix element $\langle 0 | \bar{\psi} \left(-\frac{z^-}{2} \right) \mathcal{P} \gamma^+ \psi \left(\frac{z^-}{2} \right) | \pi \rangle$

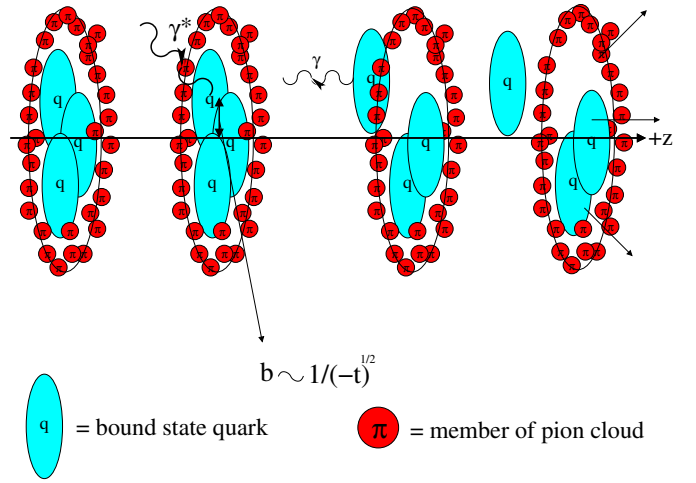


Fig. 4. Stylized picture of how striking a valence quark and creating a real photon will lead to a proton breakup

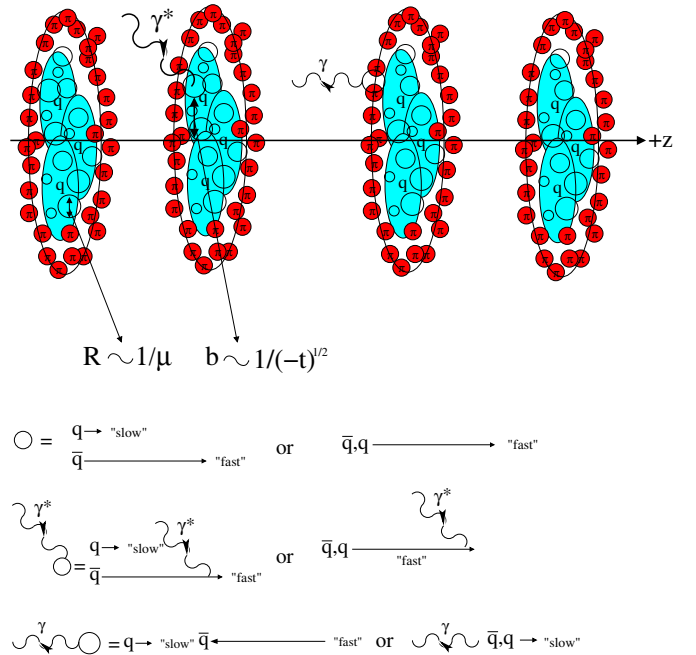


Fig. 5. Stylized picture of how DVCS proceeds through sea configurations. The empty circle corresponds to possible partonic sea configurations through which DVCS can proceed, the empty circle struck by the virtual photon corresponds either of the previous configurations interacting with the virtual photon and the empty circle emitting a real photon corresponds to the possible creation mechanism through parton annihilation or radiation

two quarks, then radiate a real photon which moves in the $-z$ direction. After radiating the photon, the quark will then become “soft” i.e. has no large momentum components. The transition matrix element i.e. the overlap integral, between an initial state with n^2 bound collinear or “fast” quarks to a final bound state with $n - 1$ collinear quarks and one soft or “slow” quark is suppressed. This is due to the probability of two collinear and one “soft”

² $n = \#$ of quark Fock states with large momentum fractions

quark forming a proton in the final state being linearly suppressed with the relative light-like separation or in momentum space with the momentum fraction, $X - \zeta$, of the “slow” quark (see (53) of [29]). DVCS, however, is observed at large x_{Bj} [30] and low Q , therefore, the only alternative picture (Fig. 5) is the one where the virtual photon is not scattering on a bound state quark but rather on a q/\bar{q} from sea configurations/QCD vacuum fluctuations which are *not* relevant for the actual bound state. In these configurations the q/\bar{q} has a large + momentum fraction which is at large x_{Bj} thus making DVCS rare, matching the one from the virtual photon. In other words, the struck q/\bar{q} starts to move in the $-z$ direction and then annihilates with a “soft” ($X - \zeta \simeq 0$) \bar{q}/q from the sea into a real photon or radiates a real photon and becomes “soft”. This real photon has a large $-$ momentum i.e. moves along the $-z$ direction, as it should. None of the bound state quarks are directly involved in the reaction and therefore, it is not very difficult for the proton to stay intact. This statement can be equivalently recast in saying that the physics of the bound state itself is not disturbed by the reaction. This implies that the bound state quarks themselves will mainly be found in symmetric configurations as in DIS. Also note that for the asymmetric, “fast” \rightarrow “slow”, configurations above, there will be no large color forces since color is conserved locally through either event. The above has consequences for the quark GPD with its valence and sea part. For $X \sim \zeta$, where the configurations are asymmetric, the non-perturbative valence distribution will be suppressed compared to the inclusive case as well as the unknown part of the non-perturbative sea necessary for the bound state.

The inclusion of gluons (their contribution is suppressed by α_s) does not change the above developed picture and interpretation. To produce the required asymmetric gluon configuration, the collinear gluon, with + momentum $X \simeq O(\zeta)$, has to split into a $q\bar{q}$ pair: a hard q/\bar{q} with large + and transverse momentum, interacts with the γ^* , after which it remains hard but now with large $-$ rather than + momentum, and then annihilates with the other hard \bar{q}/q which has only large negative transverse momentum, into a real photon with only large $-$ momentum. The soft gluon $X - \zeta \simeq O(0)$ for the color matching of the collinear gluon can be absorbed/radiated from either q or \bar{q} . This will leave the proton intact since, once more, the bound state quarks are not directly involved and color is locally conserved. The reader might wonder why gluons with $X \gg \zeta$ seem not to contribute to the imaginary part of the amplitude, even though formally they do? The answer to this question is an empirical one. Formally the imaginary part of the gluon amplitude is given by

$$\begin{aligned} \text{Im } \mathcal{T}_{\text{DVCS}}^{g,V/A}(\zeta, Q^2) &= \frac{1}{N_f} \left(\frac{2 - \zeta}{\zeta} \right)^2 \\ &\times \left[\int_{\zeta}^1 dX \left[\text{Im} T^{g,V/A}(z) \left(\mathcal{F}^{g,V/A}(X, \zeta) - \mathcal{F}^{g,V/A}(\zeta, \zeta) \right) \right] \right. \\ &\quad \left. + \mathcal{F}^{g,V/A}(\zeta, \zeta) \text{Im} \int_0^1 dX T^{g,V/A}(z) \right], \quad (7) \end{aligned}$$

with an identical structure for the quark part. Note that the second term in (7) is proportional to the gluon GPD at the point ζ and this second term is usually the dominant contribution up to a $\zeta \simeq 0.1$. Furthermore, in the integral of (7), the region $X \simeq O(\zeta)$ does, contrary to expectations, contribute a fairly large part to the value of the integral. In consequence one can indeed say that for small to medium ζ the simplified picture from above is indeed the correct one.

For small x_{Bj} , the picture does only change in so far as that there are now no bound state quarks anymore which are “visible” to the probe, and DVCS definitely has to proceed via the above advocated asymmetric parton configurations which, at a non-perturbative scale, should be mainly found in the sea.

There are two things to note here; first, the above mentioned sea configurations will be very rare at low Q and any x_{Bj} , making DVCS a rare event compared to DIS, and secondly, that these sea configurations cannot directly be identified in inclusive DIS, since this would require too large a light-light separation as compared to the one allowed in DIS.

Thus, one can conclude that *first, there exist asymmetric parton configurations/correlations in the proton, not directly associated with the bound state structure of the proton. These parton correlations themselves are encoded in GPDs in the region around $X \simeq \zeta$ and can only be probed in hard exclusive reactions like DVCS.*

What happens at larger Q^2 ? Is the above picture still valid?

2.4 The origin of the asymmetric parton correlations

The final questions of the previous subsection are easily answered when considering the perturbative evolution of GPDs as Q^2 increases: Perturbative evolution i.e. the change of the GPD under a change in the renormalization or momentum scale, strongly enhances the $X \simeq \zeta = x_{Bj}$ region in the quark singlet GPD. Within the singlet, the sea is much more enhanced than the valence part, as compared to the evolution effect in forward PDFs at the same x_{Bj} (see for example [21, 22] for a detailed analysis of this phenomenon). This enhancement effect is driven by the gluon GPD which itself is not as strongly enhanced as the quark GPD, and the structure of the perturbative evolution kernels [31] favoring splitting into asymmetric configurations. This is similar to the inclusive case where the gluon PDF drives the rise of the quark sea; however, not as strong as in the GPD case at $X \simeq \zeta$. Note that the gluons responsible for the enhancement at higher Q^2 originate themselves from quarks at higher values of X and lower values of Q^2 i.e. are collinearly radiated from the non-perturbative i.e. low scale valence quarks in the proton which are found *not* in asymmetric configurations but rather in symmetric ones as encountered in DIS. Thus evolution creates more and more asymmetric correlations inside the proton as it makes a transition from $\langle p |$ to $|p' \rangle$ and hence the valence quarks at low Q^2 become more and more “dressed” at higher Q^2 (see Fig. 5) or, equivalently, their correlated, perturbative

substructure, the sea or perturbative QCD vacuum fluctuations, is more and more revealed as the scale is increased (see Sect. 2.6) making DVCS more and more likely without having to change the actual reaction mechanism. One can say then that at low Q^2 and large $X \neq \zeta$ (disregarding the t dependence for the time being) the quark GPD and the inclusive quark PDF should be the same since they are both dominated by the same type of symmetric configurations at low Q^2 . However, since the evolution is different for the GPD and PDF the two will be different at higher Q^2 . In summary, *at large Q^2 and any x_{Bj} the asymmetric parton correlations responsible for facilitating DVCS are almost exclusively perturbative in nature.*

The question of the origin of the asymmetric parton correlations at low Q^2 where perturbative evolution is either not valid anymore or its use is questionable, is more difficult to answer. They should be a non-perturbative feature of QCD vacuum fluctuations rather than the valence structure which is found in much more symmetric configurations as discussed above. Also, one might expect that non-perturbative asymmetric configurations would be suppressed since they would look like end-point configurations in a meson. At large x_{Bj} where the valence quarks of the proton dominate, the expectation would be that there are no or very few such asymmetric correlations (see Fig. 4). However, at very small x_{Bj} , when one enters the high gluon density or non-linear regime, one might still be able to answer the question from a perturbative point of view. This is true as long as the natural scale of the problem is the so-called saturation scale $Q_s = \left(\frac{x_0}{x_{Bj}}\right)^\lambda \cdot Q_0$ with $\lambda \sim 0.15-0.2$ and x_0, Q_0 some reference/normalization scales where the small x evolution starts. This means that Q_s will be large at small x_{Bj} . Saturation refers here to the effect that in the regime of large color fields the overlap of gluon wavefunctions lead to destructive interference effects which are characterized by essential non-linearities in the relevant small x_{Bj} evolution equations for the color correlators, for example dipoles (see for example [32] and references therein). These non-linearities slow down the rapid increase of the number of gluons in the nucleon as x_{Bj} decreases. This does not mean that the photon has virtuality Q_s^2 but rather that the internal scale of the gluon couplings in the system is $\alpha_s(O(Q_s^2))$, which is small at sufficiently small x_{Bj} rather than $\alpha_s(Q^2)$ which at $Q^2 \leq 1 \text{ GeV}^2$ is large. This statement deserves a further explanation since it is counter-intuitive. It is most easily understood in the color dipole model (see for example [42] and references therein) where the DVCS amplitude is given as a convolution of a virtual photon wavefunction with a dipole cross section and a real photon wavefunction. One can easily show [32] that the Q^2 dependence resides solely in the wavefunction and that the dipole cross section depends only on x_{Bj}, x_0, Q_0 i.e. Q_s . The small x evolution determines how σ_{dipole} changes as x_{Bj} decreases, *independent* of Q^2 . The scale Q_s is determined by λ which in turn is given by the relative change in $\ln(1/x_{Bj})$ of the slope of the dipole distribution in dipole size r at the point where the distribution is about $1/2$ (see [32] and references therein). To be more precise, in

the evolution equation for the color correlator, which is essentially σ_{dipole} , α_s appears underneath the convolution integral of the evolution kernel with a combination of linear and non-linear color correlators. On inspection [43,44] it turns out that the main contribution to the convolution integral stems from dipole sizes of $O(1/Q_s)$ in the case of running coupling. Contributions of larger dipoles (infra-red contributions) are suppressed by the non-linearity (this is also true for fixed coupling) and contributions from very small dipoles ($r \rightarrow 0, k_\perp \rightarrow \infty$, ultraviolet contributions) are sufficiently suppressed due to the smallness of α_s . This is not the case, by the way for the fixed coupling case. The key observation is therefore that the smallness of α_s , if Q_s is large, allows a perturbative treatment of the gluonic degrees of freedom and thus their evolution in x_{Bj} , despite that fact that the color fields are very large. Note, however, that this does not imply that the DVCS amplitude or the total DIS cross section for that matter, is entirely perturbative at small x_{Bj} . But rather that the change in σ_{dipole} with x_{Bj} is, whereas the non-perturbative information at small Q^2 resides in the photon wavefunction and in the initial condition for σ_{dipole} at x_0, Q_0 .

In the above regime, one can therefore say that asymmetric configurations again originate from perturbatively treatable gluon configurations, as at large Q^2 , though these configurations come from completely different regions of phase space and thus correspond to a different aspect of QCD vacuum fluctuations as compared to the ones at large Q^2 . Let me add a note of caution here as far as the identification of high density gluons with a gluon GPD is concerned. The non-linear, small x_{Bj} evolution does not rely on a twist expansion but rather includes *all* twists. In fact higher twist contributions provide the essential non-linearities in the evolution equations.

In summarizing one can say that *the main source of the asymmetric parton configurations are gluons originating themselves either from symmetric valence configurations at a lower scale or are part of non-perturbative QCD configurations at small x_{Bj} .*

2.5 Meson production and GPDs

If one were to consider other reactions like meson production, the situation, previously discussed, obviously changes since one does not want to produce an elementary particle which is predominantly point-like and therefore easily allows particle configuration of “infinite” extent in its creation, but rather a bound state with a “finite” size. As I will explain below, only some details are adjusted; the overall picture, however, remains unaltered.

As in DVCS in LO of perturbation theory, the imaginary part of the scattering amplitude in meson production is proportional to $\mathcal{F}(\zeta, \zeta, Q^2)$. Depending on the produced meson i.e. its quantum numbers, a particular combination or particular types of GPDs are probed in contrast to DVCS where only the quark singlet is directly probed. Therefore, the mesons act as a “GPD filter”. For example π^0 production, being a pseudo-scalar, singles out the polarized quark GPD in an unpolarized reaction [8]!

Consider the following picture of meson production, again in the infinite momentum frame: The proton moves along the $+$ direction of the light cone and is struck by a highly virtual, longitudinally polarized (so as to maintain factorization) photon, again having large $+$ and $-$ light cone momenta. In order to produce a meson there has to be the exchange of at least one gluon or equivalently the splitting of a gluon into a $q\bar{q}$ pair. These can be, in keeping with the factorization theorem for meson production [8], either hard or collinear to the proton i.e. the $+$ direction, or collinear to the produced meson i.e. the $-$ direction. We are now particularly interested in the situation when the struck collinear quark in the proton (valence or not) carries the initial momentum fraction $X \simeq x_{Bj}$ with another accompanying quark/anti-quark being “soft” i.e. $X - \zeta \simeq 0$ as in DVCS. This situation can only be achieved through the exchange of at least one hard gluon. One can also probe the gluon GPD directly, as in, for example, J/ψ production [8] at small x_{Bj} where the gluon dominates. This corresponds to the case when a collinear gluon carrying momentum fraction $X \simeq x_{Bj}$, splits into a $q\bar{q}$ pair, one of which interacts with the virtual photon and the other one with a second, “soft”, gluon. They then go on to form the meson in the final state. In both instances, one directly probes the point $X = \zeta = x_{Bj}$ in the GPD associated with a large light-like separation of operators as in DVCS.

Let me discuss the quark case first and then speak about the gluon case. When the collinear quark, which will eventually interact with the virtual photon, radiates a hard gluon, the quark itself becomes hard. We need the situation where the $+$ component of the hard gluon is small i.e. it is on or almost on mass shell, in exact analogy to the quark connecting the two photon vertices in DVCS in Fig.3 for the situation $X \simeq \zeta$ as explained in Sect.2.3. The quark remains hard, and, at the photon–quark vertex, the struck quark starts to move along the $-$ direction, since the $+$ components of the virtual photon and quark cancel. The gluon now splits either into a $q\bar{q}$ pair with the anti-quark carrying large $-$ momentum or it hits a “soft” anti-quark in the proton transferring its large $-$ momentum. In both instances the soft quark will be associated with the proton. In order to keep the proton intact, the struck collinear quark could not have been a valence quark since there would be no other collinear i.e. “fast” quark to replace it, only a “soft” i.e. slow one. Thus it must have come from a non-valence-like configuration leaving only the sea. In this way, the situation is analogous to the DVCS case. Hence, the interpretation of the exact particle configurations probed in the GPD in meson production compared to DVCS for $X \simeq x_{Bj}$ does not change for the case of quark scattering. What happens when we have a collinear gluon as mentioned above?

The situation is quite similar to the quark case. To produce an asymmetric configuration, the collinear gluon has to split into a hard $q\bar{q}$ pair where either the hard q or \bar{q} has to go on or near mass shell only carrying large $-$ momentum, implying that the initial, collinear gluon has a $+$ momentum fraction $X \simeq \zeta$, and then radiating a “soft” gluon required to match the color of the initial

gluon. Again we have the same situation as in the quark case and therefore the same interpretation, except that we have now the gluon GPD rather than the quark GPD at $X = \zeta$ as already stated above. The origin of these asymmetric gluon configurations is the same as the one for the quark case as explained in Sect.2.4.

The fact that the interpretation about dominant particle configurations encoded in the GPD does not change in going from DVCS to meson production means that GPDs are indeed universal objects as already proven to all orders in the factorization theorems [6,8]. However, it is nice to see how this universality emerges from the simple physical picture above. Again, I would like to stress that this picture of dominant particle configurations in meson production is only valid if the imaginary part of the scattering amplitude is larger than the real part. In fact, for the real part where the regions $X \gg x_{Bj}$ and $X \ll x_{Bj}$ are very important, valence quarks and symmetric gluon configurations do play an important role. This is due to the fact that the region of phase space where the exchanged gluon or q and \bar{q} is hard, becomes large. It is also clear that, as the mass of the produced vector meson or Q^2 increases, it starts to act in a similar fashion to a point particle i.e directly emerges from the hard scattering space-time point.

The above also shows that the questions one asks of the proton in DIS and hard, exclusive reactions are different. In DIS, on the one hand, one asks the question if there are partons with large or small momentum fractions in the proton, in hard, exclusive reactions, on the other hand, one asks the much more specific question of how the partons in the proton must conspire to make the reaction happen and therefore one obtains a much more specific answer. One can then conclude that *there exist asymmetric parton configurations/correlations in the proton, the exact nature of which can only be probed in hard exclusive reactions like DVCS or meson production. These parton correlations are encoded in a GPD in the region around $X \simeq \zeta$.*

2.6 The t and Q^2 dependence of GPDs

Up until now, I have neither talked about the role of the t dependence nor of the precise meaning of Q^2 or more precisely the renormalization scale μ^2 . In [33], a beautiful exposition of the physical meaning of these two variables for GPDs has been given (see also [34]) which I will only briefly reiterate: The scale μ^2 defines from what scale, or, in space-time, from what resolution in the transverse plane, onwards one can speak of several partons or just one parton. In other words, the better the resolution $1/Q \sim 1/\mu$ of the probe, the more partons or substructure of one parton one can observe (see Fig. 5). As μ defines the resolution of the parton in the transverse plane, the t dependence gives the relative transverse position of the probed parton correlation with respect to the proton (see Fig. 4). If $\mu^2 \simeq -t =$ several GeV^2 , the exact meaning between resolution and position becomes lost, including the above simple picture of DVCS and meson production, since the hierarchy of scales necessary for a factorized approach to these processes is lost and hence also its simple physical picture.

In contrast, in the case of $\mu^2 = Q^2 \gg -t$, one has a very interesting picture emerging (see Fig. 5): since t is up to corrections of $O(M_N^2 \zeta^2)$, which are very small, equal to $-(p_\perp - p'_\perp)^2$, the relative transverse momentum difference between initial and final state, a small t corresponds to a large distance in the transverse plane from the proton “center” and large t to a small distance. Here “center” is meant with respect to the relative transverse positional difference between initial and final state. The question which arises now is where, relative to this “center”, the asymmetric parton correlations take place.

As far as the perturbatively generated correlations having a resolved size of $O(1/Q)$ in the transverse plane are concerned, they will take place closer to the “center”, since they are associated with the valence quarks through evolution and those have to be situated well within the proton radius, $r_p \sim 1$ Fermi. The non-perturbative correlations have to be more clearly separated from the “center” of the proton. The reason for this lies in the very fact that they cannot be associated with the bound state structure as shown above and therefore they will have to be situated in the “pion cloud”, for lack of a better word, at the “edge” of the proton.

The emerging three dimensional picture of the asymmetric parton configurations as well as their symmetric “parents” can be stated as follows: The asymmetric parton configurations necessary to facilitate hard, exclusive reactions are basically located “inside” of the proton as it makes a transition from $\langle p |$ to $| p' \rangle$ during the reaction, with the non-perturbative configurations towards the edge and the perturbative configurations more towards the “center” but very spread out on the light cone. For example, at the average t in DVCS on the proton of HERMES of about -0.2 GeV^2 , these configurations are located only about 0.4 Fermi away from the “center”, clearly “inside” the proton charge radius $r_p \sim 1$ Fermi (only for a $t < -0.04 \text{ GeV}^2$ would they be located “outside” of the proton charge radius r_p). Since we restrict our considerations to the region of $-t \leq 1 \text{ GeV}^2$, the relative distance to the “center” is never closer than about 0.2 Fermi.

One can now also understand why the cross section of hard, exclusive processes drops when t is increased and how this depends on x_{Bj} and Q^2 . To do this, consider the following (see Fig. 5): At low Q^2 and fixed x_{Bj} , the main source of the asymmetric configurations will not yet be perturbative collinear parton splitting as at large Q^2 , but rather some non-perturbative property of QCD vacuum fluctuations. This means that, at low Q^2 , as one approaches the “center” of the proton i.e. as t increases, the number of asymmetric configurations suitable to facilitate a hard, exclusive event should drop since the non-perturbative configurations sit at the edge rather than in the “center”, while at the same time the perturbative configurations as part of the substructure of the valence quarks, are not as well resolved yet as at higher Q^2 and hence less than at large Q^2 . In consequence, the average number of asymmetric configurations available to the reaction is less at larger t than at smaller t , and as a consequence, the cross section drops faster with the increase in t at low Q^2 than at large Q^2 . Furthermore,

as x_{Bj} decreases i.e. the energy increases, the number of gluons from which asymmetric correlations can originate will also increase, since more and more gauge fields will become “frozen” in the light cone time z^+ (see [32] and references therein for details) and can thus serve as a source. This means that the cross section will drop faster with increasing t at larger x_{Bj} than at smaller x_{Bj} . Since the evolution in x_{Bj} is less dramatic than in Q^2 (see again [32] and references therein), the effect on the t dependence will be less.

These observations are borne out both by the observations made in [35] where a Q^2 dependent but basically x_{Bj} independent slope gives very good agreement, within the experimental errors, between the DVCS data and NLO QCD calculations and by experimental measurements (see for example [47] and references therein).

3 Going beyond the nucleon: Qualitative predictions from the above picture

The above considerations are not limited to a nucleon target but are also valid for example for a nuclear target. There are some interesting consequences emerging from the above considerations: The fact that the same large light-like distances are involved in conventional PDFs for $x_{Bj} \rightarrow 0$ and in GPDs for $X \simeq \zeta$ together with the observed enhancement of this region through perturbative evolution, suggests that for the same x_{Bj} of the process, *GPDs probe the configuration content of the proton and its effect on the QCD vacuum at relatively smaller momentum fractions than PDFs*. This is borne out by the analysis carried out in [35] which shows that a good GPD input capable of describing all available DVCS data [30, 36, 37] in a NLO QCD analysis is obtained by using conventional forward PDFs at a momentum fraction X shifted to a smaller value by an amount of $O(\zeta)$. This in turn implies the following.

- (1) Earlier onset of saturation effects in DVCS observables dominated by the imaginary part of the scattering amplitude as compared to inclusive observables. This is particularly true for nuclear targets since saturation is a strongly x_{Bj} dependent phenomenon [38]! A concrete prediction would be the presence of geometric scaling in the $\gamma^* p$ DVCS cross section in either ep or eA scattering up to an x_{Bj} where it normally would break down in $F_2^{p,A3}$.
- (2) Nuclear shadowing corrections for DVCS should set in at larger values of x_{Bj} as compared to the inclusive case. Moreover, at comparable values of x_{Bj} , the nuclear shadowing corrections should be stronger in DVCS compared to DIS. Since nuclear shadowing is only a weak function of x_{Bj} except for the transition region between $0.01 < x_{Bj} < 0.1$ (see for example [40]), the enhancement effect would probably be mainly visible in this region [41].

³ Munier and Wallon [39] demonstrate geometric scaling in exclusive J/ψ production with different scaling curves for different impact parameter i.e. t

(3) Since varying t changes the relative transverse position at which the target is probed, it will allow one to scan through the “grey” region, where non-linear perturbative QCD is still applicable, and the “black” or total absorption region of the target. In these two regions, the target behavior will be qualitatively different and this difference should be reflected in different geometric scaling curves for different values of t (see the above footnote 3). I do not claim here that DVCS in the black disc limit is very different from DIS in this limit – quite on the contrary [42]. However, the t dependence allows one to discern the discrepancy between two regions of different target behavior.

These predictions could be verified at the future EIC with its high luminosity both for ep and eA scattering, as well as at HERA III with nuclei in the HERA ring or a dedicated, high luminosity, fixed target experiment.

Furthermore, the fact that one cannot really probe the bound state quark distributions at $X = \zeta$ and leave the proton intact, leads one to conclude that as $X \rightarrow \zeta$ the non-perturbative unpolarized valence quark GPD should become small relative to the inclusive valence PDF at the same x_{Bj} or tend even to zero at the input scale. Evolution will change this and the valence GPD will start to grow also at $X = \zeta$ since higher and higher Fock states will be present in the valence GPD at higher Q^2 as previously discussed in Sect. 2.4. This prediction is supported by several model calculations. First, calculations both in the chiral-quark-soliton model [45], in the constituent quark model [46] and within a light cone wavefunction approach [29] show that the valence GPD becomes either small or vanishes at $X = \zeta$. In the chiral-quark-soliton model, for example, the contribution to the flavor singlet of the discrete Dirac spectrum is identified with the bound state quark structure – both valence and sea – whereas the continuum part is identified with the pion field itself [45] or what I termed non-perturbative QCD vacuum fluctuations. The continuum part rapidly changes behavior from an increasing to a decreasing function which is essentially 0 at the crossover $X = \zeta$. This is easily explainable if one remembers that the asymmetric $q\bar{q}$ fluctuations from the non-perturbative vacuum at a low scale correspond to endpoint contributions in the pion or meson wavefunction which are suppressed. Note that the continuum contribution is C -even and thus the individual flavor contributions enter the DVCS amplitude with the square of their respective charges. The bound state quark distribution has both a C -even and C -odd part, where the flavor decomposed C -even part contributes to the DVCS amplitude. In order to replicate the value of this distribution at $X = \zeta$ as well as its functional behavior (see Fig. 2 of [45]), the value of the C -even and C -odd parts at $X = \zeta$ should be both positive, but smaller than the value of the total bound state quark distribution. This means that both the C -even and C -odd or valence distribution in the DGLAP region have essentially the same functional behavior as the total distribution. This means that the sum of the C -even distribution from the continuum and discrete part as well as the valence distribution yield a falling distribution towards $X = \zeta$ at a non-perturbative scale,

as I advocate. In other words, the required configurations for DVCS are rare at a non-perturbative scale.

Secondly, since $X = \zeta$ corresponds to large light-like separations as in the inclusive case for $x_{Bj} \rightarrow 0$, one might expect that the non-perturbative valence quark GPD actually vanishes at $X = \zeta$ as the forward valence quark PDF vanishes for $x_{Bj} \rightarrow 0$. Experimentally, this could be verified in principle through a flavor separation in νp DVCS at the COMPASS experiment at very low Q^2 with the two huge caveats of unknown higher twist and a large BH contribution at very low Q^2 and large x_{Bj} .

The slope of the t dependence for small values of t in DVCS at low $Q^2 \sim$ a few GeV^2 should be larger than the one for light meson production for the same kinematics, whereas at large Q^2 , the two slopes should be the same as stated in factorization theorems [6, 8]. The reason for this is quite simple in the region of x_{Bj} and Q^2 where the imaginary part of the amplitude dominates: In meson production, as pointed out above, both asymmetric quark and gluon configurations couple to the reaction with equal strength. Whereas in DVCS the coupling strength of the quark and gluon correlations are very different, α and $\alpha\alpha_s$, respectively. It is important to note that I do not assume that the asymmetric quark and gluon configurations have a different spatial distribution in the transverse plane.

Why is the difference in coupling strength important in this case? Because of the difference in coupling strength compared to meson production the slope in t for DVCS at low Q^2 is quark dominated while in meson production it is a priori a mixture of quarks and gluons. If quarks and gluons had the same t slope, then the difference in coupling strength would not matter since percentage wise the amplitude for DVCS and meson production would change the same way in t and the t slopes would be independent of Q^2 . If gluons had a larger slope in t than quarks, one would expect that for large Q^2 , due to the mixing of quarks and gluons under perturbative evolution which equilibrates the slopes of quarks and gluons, the slope for DVCS or meson production would increase with Q^2 since the slope for quarks would increase. Both of the above assumptions are not what the data indicate (see for example [35, 47]). Rather than a constant slope or an increase, one observes a decrease of the slope with an increase of Q^2 . The fact that the smallest slope is measured in J/ψ photoproduction which is essentially only sensitive to the gluon GPD, tells us that quarks and gluons have not only different slopes in t at $Q^2 \simeq M_{J/\psi}^2$ which corresponds to small transverse distances, but that the slope for gluons is smaller than that for quarks. Going to even lower scales, the difference in slope can only increase rather than decrease because of the evolution argument. Note once more that I do not refer to any particular difference between spatial distributions of quarks and gluons.

If one were to take $x_{Bj} \leq 0.01$, $Q^2 \simeq 2 \text{ GeV}^2$, integrate out t and further assume, for simplicity, that the gluon amplitude which enters both DVCS and meson production in this kinematic region with a $-$ sign, is between 30–50% of the quark amplitude at low Q^2 modulo coupling effects, then it is a simple exercise to show that the effective t slope

for DVCS is larger than for meson production. Furthermore, it is immediately clear that the difference depends on the relative difference in coupling strength between quarks and gluons in DVCS and meson production.

Taking the quark slope to be about 8 and for gluons to be about 4 seems to be not unreasonable. Furthermore take $\alpha_s \simeq 0.3$ and the gluon about 50% of the quark. The effective slope for DVCS i.e. for the square of the amplitude assuming a t dependence in the amplitude of $e^{B_{q,g}t/2}$ for small t , is then about $16/1.79$ compared to $16/2$ for light meson production which will be mainly ρ production in this kinematic range. Taking the ratio of effective slopes of meson production to DVCS gives about 0.8. The difference in the ratio from 1 is entirely due to the difference in the coupling strength between quarks and gluons in DVCS and meson production respectively.

At large Q^2 , on the other hand, where there will be many suitable configurations, originating almost exclusively from gluons, this difference in coupling strength becomes unimportant due to the very large number of suitable configurations which leads to an equilibration of quark and gluon slopes. The conclusion for low Q^2 is supported by the findings in [35] where a larger slope for DVCS at relatively low $Q^2 \sim 2-4 \text{ GeV}^2$ was required to obtain a good agreement between data and theory than in the case of, for example, ρ^0 production [47] with a ratio of the effective slopes of about 0.7–0.8. That the t slopes for quark and gluons equilibrate at large Q^2 and become universal as predicted by factorization is seen in the effective slope for ρ production [47] rapidly approaching the one for J/ψ production with an increase in Q^2 , but not going below that value for even larger Q^2 .

4 Conclusions

To summarize once more, I have presented a concise, simple and intuitive picture of what GPDs mean in the sense of carrying new information about the three dimensional (two transverse and one light cone dimension) structure of nucleons (more precisely nucleon to nucleon transitions) compared to inclusive parton distributions or form factors. To achieve this I have developed a simple picture through which type of particle configurations encoded in the GPDs, DVCS and meson production proceed and that these configurations can only be correctly identified in exclusive reactions. These configurations originate mainly from symmetric quark configurations through perturbative evolution. Furthermore, based on this picture, I conclude that the unpolarized valence quark GPD at a non-perturbative scale should be either small compared to an inclusive valence PDF at the same x_{Bj} , or vanish near the crossover point between the ERBL and the DGLAP region. I have also made verifiable, qualitative predictions for DVCS and meson production in ep and eA collisions such as an early onset of saturation, different geometric scaling curves for different t values, determining the sizes of the “grey” and “black” areas of the target, stronger nuclear shadowing corrections in the transition region $0.01 < x_{Bj} < 0.1$ and a difference in the slope of the t dependence at low Q^2

between the two processes, using the above picture. These predictions/conclusions are already partially supported by both experimental as well as theoretical observations.

Acknowledgements. I would like to thank Nikolai Kivel, Mark Strikman and Christian Weiss, for useful discussions as well as Moskov Amarian, Vladimir Braun, Einar Gardi, Mark Strikman, and Heribert Weigert for reading the manuscript. This work was supported by the Emmi-Noether grant of the DFG FR-1524/1-2.

References

1. M. Ciafaloni, Nucl. Phys. B **296**, 49 (1988); S. Catani, F. Fiorani, G. Marchesini, Phys. Lett. B **234**, 339 (1990); Nucl. Phys. B **336**, 18 (1990); G. Marchesini, Nucl. Phys. B **445**, 49 (1995)
2. D. Müller et al., Fortschr. Phys. **42**, 101 (1994)
3. X. Ji, Phys. Rev. D **55**, 7114 (1997)
4. X. Ji, J. Phys. G **24**, 1181 (1998)
5. A.V. Radyushkin, Phys. Rev. D **56**, 5524 (1997)
6. J.C. Collins, A. Freund, Phys. Rev. D **59**, 074009 (1999)
7. M. Diehl, T. Gousset, B. Pire, J.P. Ralston, Phys. Lett. B **411**, 193 (1997)
8. J.C. Collins, L. Frankfurt, M. Strikman, Phys. Rev. D **56**, 2982 (1997); S.J. Brodsky, L. Frankfurt, J.F. Gunion, A.H. Mueller, M. Strikman, Phys. Rev. D **50**, 3134 (1994)
9. J. Bartels, M. Loewe, Z. Phys. C **12**, 263 (1982)
10. M.V. Polyakov, C. Weiss, Phys. Rev. D **60**, 114017 (1999)
11. A. Freund, Phys. Rev. D **61**, 074010 (2000)
12. K. Goeke, M.V. Polyakov, M. Vanderhaeghen, Prog. Part. Nucl. Phys. **47**, 401 (2001)
13. M. Diehl, T. Gousset, B. Pire, O. Teryaev, Phys. Rev. Lett. **81**, 1782 (1998)
14. S.J. Brodsky, F. Close, J.F. Gunion, Phys. Rev. D **6**, 177 (1972); Phys. Rev. D **6**, 2652 (1972)
15. A. Freund, M. McDermott, Eur. Phys. J. C **23**, 651 (2002)
16. A.V. Belitsky, D. Müller, A. Kirchner, Nucl. Phys. B **629**, 323 (2002)
17. A.V. Belitsky, D. Müller, Nucl. Phys. A **711**, 118 (2002)
18. L. Frankfurt, M.V. Polyakov, M. Strikman, Phys. Rev. D **60**, 014010 (1999)
19. J.P. Ralston, B. Pire, Phys. Rev. D **66**, 111501 (2002)
20. K.J. Golec-Biernat, A.D. Martin, Phys. Rev. D **59**, 014029 (1999)
21. L. Frankfurt et al., Phys. Lett. B **418**, 345 (1998), Erratum **429**, 414 (1998); A. Freund, V. Guzey, Phys. Lett. B **462**, 178 (1999)
22. A. Freund, M. McDermott, Phys. Rev. D **65**, 074008 (2002)
23. A.V. Radyushkin, Phys. Lett. B **449**, 81 (1999); I.V. Musatov, A.V. Radyushkin, Phys. Rev. D **61**, 074027 (2000)
24. A.V. Belitsky, D. Müller, L. Niedermeier, A. Schäfer, Nucl. Phys. B **546**, 279 (1999); Phys. Lett. B **437**, 160 (1998); A.V. Belitsky, B. Geyer, D. Müller, A. Schäfer, Phys. Lett. B **421**, 312 (1998)
25. A.V. Belitsky et al., Phys. Lett. B **510**, 117 (2001)
26. A. Freund, M. McDermott, Phys. Rev. D **65**, 056012 (2002)
27. T. Schäfer, E.V. Shuryak, Rev. Mod. Phys. **70**, 323 (1998), D. Diakonov, hep-ph/0212026
28. A. Freund, M. McDermott, Phys. Rev. D **65**, 091901 (2002)

29. M. Diehl, T. Feldmann, R. Jakob, P. Kroll, Eur. Phys. J. C **8**, 409 (1999)
30. HERMES Collaboration, A. Airapetian et al., Phys. Rev. Lett. **87**, 182001 (2001); CLAS Collaboration, S. Stepanyan et al., Phys. Rev. Lett. **87**, 182002 (2001)
31. A.V. Belitsky, A. Freund, D. Müller, Nucl. Phys. B **574**, 347 (2000)
32. H. Weigert, Nucl. Phys. A **703**, 823 (2002)
33. M. Diehl, Eur. Phys. J. C **25**, 223 (2002)
34. M. Burkardt, Phys. Rev. D **62**, 071503 (2000), hep-ph/0207047
35. A. Freund, M. McDermott, M. Strikman, Phys. Rev. D **67**, 036001 (2003)
36. H1 Collaboration, C. Adloff et al., Phys. Lett. B **517**, 47 (2001)
37. ZEUS Collaboration, Measurement of the deeply virtual Compton scattering cross section at HERA, contributed paper (abstract: 825) to ICHEP2002 (Amsterdam, July 2002)
38. A.M. Stasto, K. Golec-Biernat, J. Kwiecinski, Phys. Rev. D **62**, 094006 (2000)
39. S. Munier, S. Wallon, hep-ph/0303211
40. L. Frankfurt, V. Guzey, M. McDermott, M. Strikman, JHEP **0202**, 027 (2002)
41. A. Freund, M. Strikman, preprint in preparation
42. L. Frankfurt, V. Guzey, M. McDermott, M. Strikman, Phys. Rev. Lett. **87**, 192301 (2001)
43. H. Weigert, K. Rummukainen, preprint in preparation
44. A. Freund, E. Gardi, H. Weigert, preprint in preparation
45. V.Yu. Petrov, P.V. Pobylitsa, M.V. Polyakov, I. Boernig, K. Goeke, C. Weiss, Phys. Rev. D **57**, 4325 (1998)
46. S. Scopetta, V. Vento, Eur. Phys. J. A **16**, 527 (2003)
47. ZEUS Collaboration, Exclusive and proton-dissociative electroproduction of ρ^0 mesons at HERA, contributed paper (abstract: 818) to ICHEP2002 (Amsterdam, July 2002)